

Influence of Arc Current on Surface Properties and Corrosion Resistance of AlCrN Coatings Deposited by Multi-arc Ion Plating

Sheng Zhu¹, Yongfa Qin^{1,*}, Hui Mei¹

School of Mechanical Engineering, Yangzhou University, Yangzhou 225127, China

*E-mail: qinyongfa@yzu.edu.cn

Received: 8 February 2020 / Accepted: 27 March 2020 / Published: 10 May 2020

High aluminum-content AlCrN (Al : Cr =70:30) coatings are deposited with various arc currents using multi-arc ion plating (M-AIP) technique. The relationships between arc currents and coating properties were studied. The microstructures and morphologies of the coatings are tested by X-ray diffraction (XRD), scanning electron microscope (SEM), energy dispersive X-ray spectroscopy (EDX) and surface profilometer, combined with potentiodynamic polarization curves of 3.5-wt% NaCl solution. Results show that the intermetallic phase turns to the fcc structure as the arc current increased, and more substrate phases can be observed. As the arc current increased, metal particles and droplets on the coating surfaces are gradually removed, and the surface roughness decreases. Potentiodynamic polarization curves show that the corrosion resistance of the AlCrN coated samples is obviously improved with the arc current increasing from 120 A to 180 A. The increase of the corrosion potential was about 120 mV and the reduction of the corrosion current with an order of magnitude.

Keywords: AlCrN; Corrosion resistance; Arc current; Multi-arc ion plating

1. INTRODUCTION

Due to its excellent comprehensive mechanical properties and low cost, 45 steel has been widely used in machinery manufacturing industry [1-3]. The surface phenomena, such as the corrosion, are the main concerns of industrial applications that determine the performance and the life of 45 steel components. Piston rods of automotive shock absorbers are usually made of 45 steel. The piston rod is an integral part of the shock absorber, and its surface properties and quality not only determine the service life of the shock absorber but also affect the safety comfort. Piston rods are used under severe conditions (such as hydraulic oil and tensile stress) for a long time. They will suffer various forms of corrosion under static and dynamic mechanical loads [4]. During driving, the shock absorber is needed to operate stably. Thus it is significant to minimize the degree of corrosion.

Physical vapour deposition (PVD) is a kind of standard and effective coating method to improve the mechanical surface properties. It is a technique of material transfer by using physical process, transfers atoms or molecules from the target to the substrate surface, and sprays some particles with special properties (such as high strength, wear resistance, corrosion resistance, etc.) on the substrate so that it has better performance [5]. PVD is with a series of advantages, such as fast deposition speed, low deposition temperature, compact structure and no pollution. The methods of PVD include vacuum evaporation, sputtering, ion plating (hollow cathode ion plating, hot cathode ion plating, arc ion plating, active reaction ion plating, etc.) [6, 7]. Among them, multi-arc ion plating (M-AIP) is a kind of ion plating technique which with the evaporation source of cathode arc discharge. It has a quite high deposition rate and a very high separation rate of the coating material. M-AIP is commonly used for AlCrN coatings [8].

In recent years, some studies have improved the surface properties of the substrate by coating technology. Chromium nitride and other non-ferrous metal coatings protect the coating surface from friction and abrasion, and have excellent corrosion and fatigue resistance [9, 10]. Chen et al. [11] studied wear performance of CrN coating on 316L stainless steel surface in liquid sodium by using self-made reciprocating friction meter for the first time. This study guided the design of coatings serving in liquid sodium environment; Wan et al. [12] used two methods to study the corrosion resistance and fatigue wear of CrN coating on piston ring. The results showed that fatigue wear would lead to cracking and spalling of CrN coating; Kuma et al. [6] used PVD technique to deposit AlCrN coating on Al₂O₃/TiCN ceramic blades with different thin film thickness. The results showed that when the coating thickness was 3 μm , the Al₂O₃ / TiCN composite ceramic blade has the best turning performance; Chen et al. [13] deposited AlCrN coating on SKD 11 cool-work tool steel by using PVD method. The relationships between PVD deposition temperature and coating structure, mechanical properties and tribological properties were discussed; Mo et al. [14] researched the performance of CrN, AlCrN, and AlTiN coatings on cemented carbide substrates by multiple-arc PVD technique through cyclic impact wear and microscale wear tests. This result showed that AlCrN coating has better impact wear resistance and wear resistance than others. In summary, AlCrN coatings have better surface properties than CrN coatings. Because of the formation of wear-resistant by friction chemical reaction between Cr and Al, it can effectively protect AlCrN coating from damage [15].

The higher the aluminum content, the better the oxidation resistance and wear resistance of AlCrN coating [16, 17], Cr-Al-N coating can maintain more than 70% aluminum content without changing the structure of AlCrN. High-aluminum AlCrN coating has become a subject of increasing concern due to its excellent properties [18, 19]. This alloy coating has many advantages, such as high hardness, wear resistance, corrosion resistance, etc. Therefore, the alloy coating can improve the surface mechanical properties and wear resistance of 45 steel without reducing the matrix properties of 45 steel, which is of great significance in actual production [6, 20].

In this study, the high aluminum-content AlCrN coatings were prepared by M-AIP on 45 steel substrates at various arc currents in Part 2. The effects of arc current on phase structures, surface morphology, surface roughness and the corrosion resistance of the AlCrN coatings were analyzed. The results are discussed and explained in Part 3, and conclusions are summarized in Part 4.

2. EXPERIMENTAL

2.1 Specimens and Coating deposition

Table 1. Chemical composition of 45 steel

Element	C	Si	Mn	Cr	Ni	Cu	Fe
Content (wt. %)	0.45	0.27	0.6	0.2	0.24	0.15	Balance

In this study, the substrate material is the 45 steel (chemical composition is shown in Table 1), which was cut into 10 mm × 10 mm × 3 mm sample. All substrates were polished to a surface roughness of about 0.04 μm R_a and then washed in ethanol for 15 minutes with an ultrasonic cleaner, dried with blower and then was put into a furnace. The coatings were deposited by M-AIP system, which includes cathode Cr targets (99.9% purity) and AlCr targets (70 at.% Al, 30 at.% Cr, 99.9% purity). Before the deposition begins, the substrates were preheated to 380 °C and then kept for 2 hours. Then, the argon was pumped into the furnace chamber until the pressure reaches 4×10^{-3} Pa, and all samples were cleaned for about 25 minutes with a bias of - 800 V in the argon plasma. The power supply was then turned on, and the sample was bombarded with target ions for 10 minutes, to enhance the adhesion between coating and substrate. After deposition, in order to avoid sample oxidation, the sample should be cooled to room temperature in a vacuum and then taken out. The processing parameters of M-AIP technique in preparing AlCrN coating are shown in table 2 during the process of coating deposition.

Table 2. Processing parameters of M-AIP technique in preparing AlCrN coating

Parameter	Value
Bias/V	-90
Target material	Al(70%)、Cr(30%)
Sedimentary pressure/Pa	0.6
Sedimentary gas	N ₂
Deposition time/min	140
Deposition temperature/°C	380
Arc current/A	120、150、180

2.2 Characterization methods

The microstructure of the samples was characterized by X-ray diffraction (XRD) and scanning electron microscopy (SEM). The surface and cross-sectional morphologies were investigated by Field Emission Scanning Electron Microscope (FE-SEM, S-4800, and 15 kV) and energy dispersive spectrometer (EDX, 20 kV). The crystal research of the AlCrN coatings was analyzed by an X-ray diffractometer (XRD, Bruker D8 advance) with Cu-K α radiation, with a scan step of 0.5°. The 2 θ range was 30°-80° with a scan rate of 5° / min.

2.3 Electrochemical measurements

The corrosion behavior of the AlCrN coatings was studied on an electrochemical workstation (INTERFACE 1010E). The reference electrode was saturated calomel electrode (SCE), and the counter electrode is platinum foil. The experiment was carried out in 3.5 at.% NaCl aqueous solution. The experimental area of the sample is about 1cm^2 . After the open circuit potential (OCP) was stabilized, the potential polarization studies were performed. All potential polarization researches were conducted after the open circuit potential (OCP) was stabilized. Before this test, the samples in the solution for 30 minutes to ensure that the samples are completely wetted. The polarization curves (E/I) were obtained by from a potential of -250 mV to 800 mV respect to the SCE with a scan rate of 1 mV / s.

3. RESULTS AND DISCUSSION

3.1 Phase structures

The typical XRD patterns of 120 A, 150A and 180A arc current deposited AlCrN coatings are shown in Fig. 1. Several peaks can be observed which were related to the fcc structure of Cr(Al)N and the intermetallic phase Al_8Cr_5 [21-23], and some substrate phases were also detected. There is no impurity peak can be observed, which indicates that the deposited AlCrN coatings have higher purity. With the increase of arc current, the peak strength of about $2\theta=42.3^\circ$ referred to intermetallic compounds decreases, and the peak strength of about $2\theta=31.54^\circ$ and 48.34° related to (Al) N of fcc structure increases. The results indicate that the increase of arc current causes more AlCrN. Meanwhile, the formation of intermetallic compounds is less, which may be due to the decrease of the average free path due to the increase of arc current [24]. Moreover, the probability of the collisions between ions and gas atoms occurred is higher, which is more helpful to the transition from Al_8Cr_5 to AlCrN. With the increase of arc current, the phase of the substrate increases gradually, which may be due to the thinner coating prepared by a higher arc current, which makes the X-ray penetrate the coating more easily. EDX analyses show that the content of Al element is always higher than that of Cr element during deposition. Therefore, when the nitrides on the coating surface are decomposed, Al_2O_3 may form. This formation of Al_2O_3 is beneficial to improve the corrosion resistance of AlCrN coatings [25, 26].

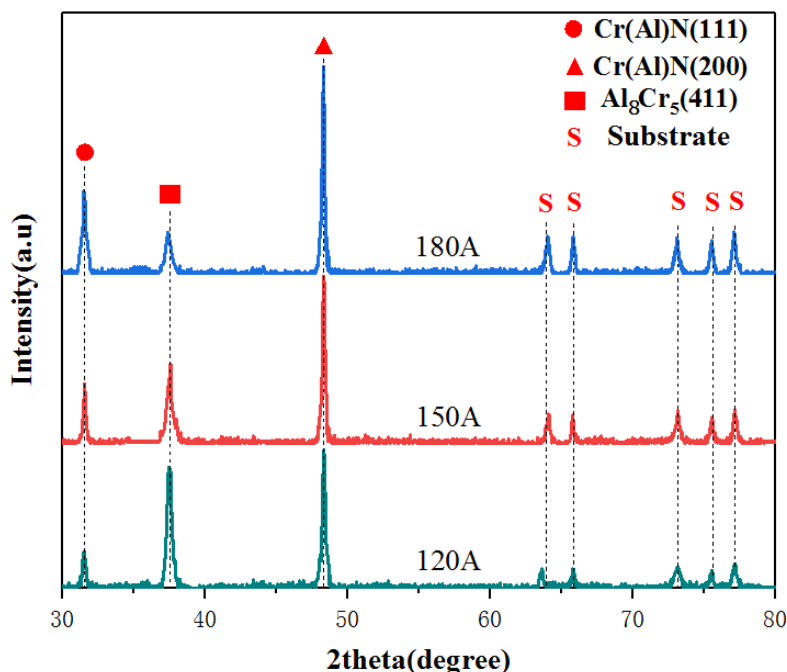


Figure 1. The XRD patterns of the AlCrN coatings, deposited at the arc currents of 120A; 150A; and 180A with a scanning rate of 5°/min and a step by step scanning length of 0.5°

3.2 Surface morphology

The SEM surface and cross-sectional morphologies of the AlCrN coatings at different arc currents are shown in Fig. 2 (a)-(f). It can be seen from the surface morphology (Fig. 2 (a), (c), (e)), there are many droplets and particles on the surfaces of the deposited AlCrN coatings. These particles are always generated during the M-AIP which come from droplets emitted by the target materials, and the collision between atoms or ions are usually caused by excessive arc current [27, 28]. Therefore, atoms or ions may aggregate into macroparticles before reaching the coating surface [24]. As shown in Fig. 2 (a), (c), (e), with arc current increases, the number and size of particles and droplets gradually decrease. It indicates that solid metal droplets are melted and then mixed into the coating, which results in many holes being filled [9]. Moreover, with the increase of arc current, the target ion emission speed is accelerated, and the aggregation of atoms or ions is reduced. The EDX surface analysis of the AlCrN coatings deposited by different arc currents is shown in Fig. 3. These particles can be observed to contain abundant Cr and Al, which means that they are composed of Cr and Al pure metal or Cr-Al alloy. With the increase of arc current, the content of Al and Cr increases. This phenomenon may be due to the improved arc current, which leads to the target emitting more ions [29].

The cross-sectional morphologies of AlCrN coatings are shown in Fig. 2 (b), (d), (f). It can be measured that the corresponding coating thicknesses with the arc current of 120, 150, 180 A is 24.6 nm, 22.1 nm, and 16.3 nm, decreasing continuously. With the increase of arc current, the binding force between the ions and substrate is enhanced to form a thinner and more uniform coating [27].

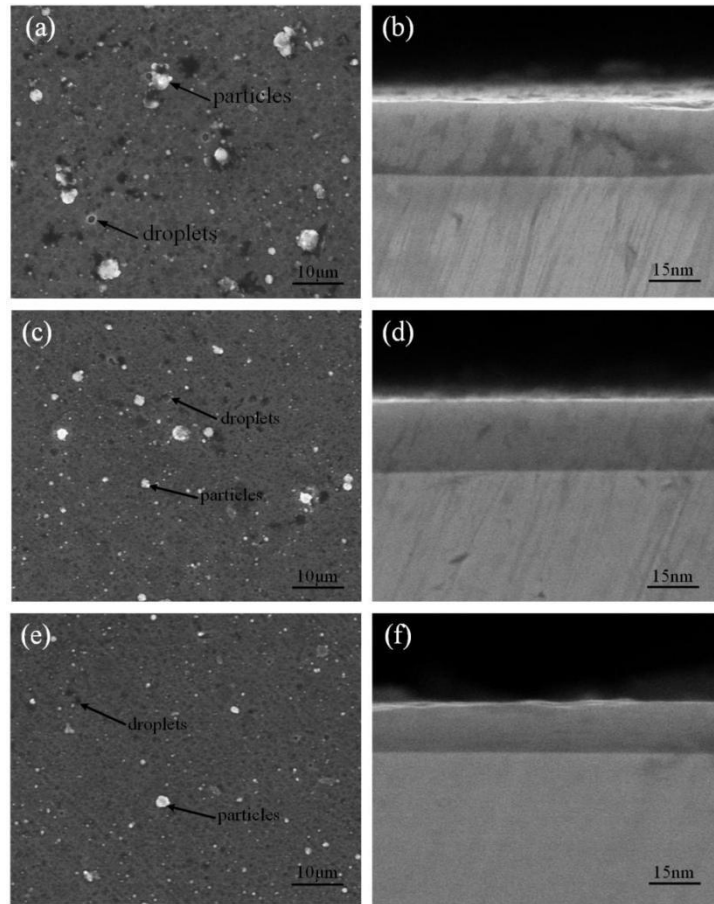


Figure 2. Surface FE-SEM and cross-sectional morphologies of the AlCrN coatings, deposited at the arc current of (a) (b): 120A; (c) (d): 150A; (e) (f): 180A.

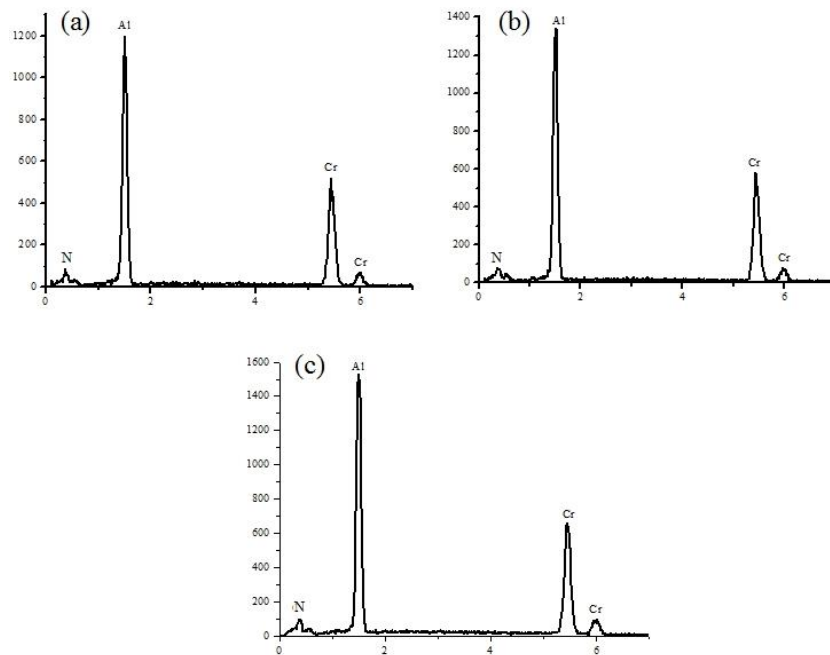


Figure 3. Elemental composition analysis of the AlCrN coatings, deposited at the arc current of (a) 120 A; (b) 150 A; (c) 180 A.

3.3 Surface roughness

The three-dimensional contours of surface roughness at different arc currents are shown in Fig.4. As shown in Fig. 4 (a), the surface of the substrate is smooth, and the polishing scratches line up. However, due to the bombardment of target ions, as shown in Fig. 4 (b) - (d), the polished scratches disappear, and the surface becomes rough, which may be caused by the intense bombardment of ions. The surface roughness values are listed in Table 3. The results show that surface roughness increases after deposition by changing roughness from 39.543 nm R_a for grinded surface to 98.206 nm R_a after coating deposition. As shown in Table 3, surface roughness reduced from 98.206 nm R_a to 51.463 nm R_a with increasing the arc current from 120 A to 180 A, which may due to the higher arc current enhancing the binding force between the target ions and the substrate. The surface roughness has a great influence on the wear resistance and corrosion resistance of the coating, and the thinner the coating thickness, the lower surface roughness and the higher corrosion resistance [30].

Table 3. Surface roughness analysis of AlCrN coatings deposited at different arc currents

Specimen	Substrate	120A	150A	180A
R_a / nm	39.543	98.206	91.687	51.463

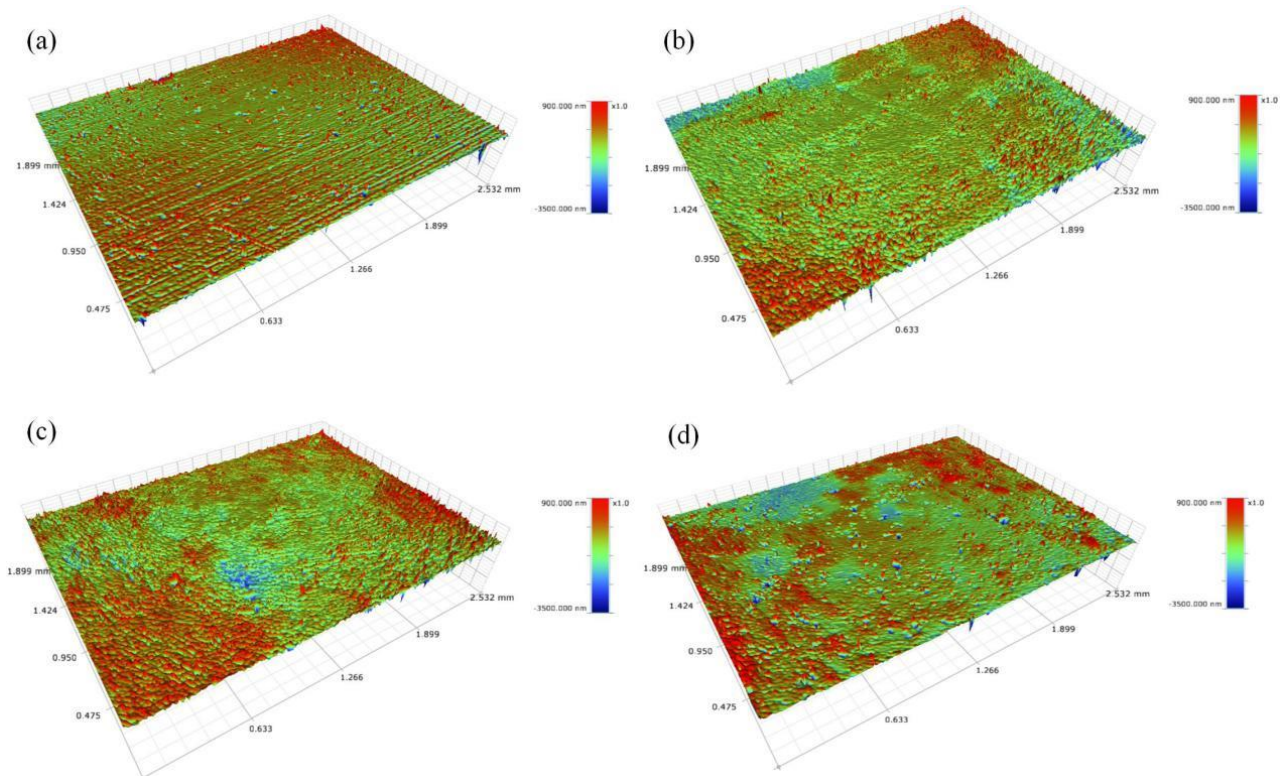


Figure 4. Surface roughness analysis of the AlCrN coatings, deposited at the arc current of (a) substrate; (b) 120 A; (c) 150 A; (d) 180 A.

3.4 Corrosion behavior

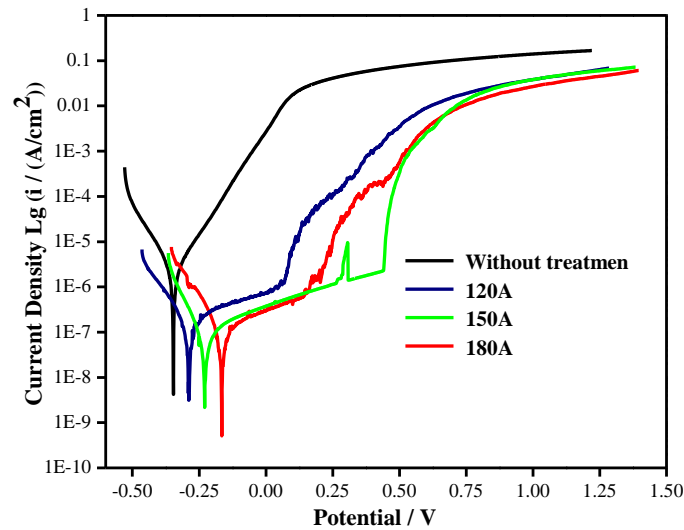


Figure 5. Potentiodynamic polarization curves of the AlCrN coatings corroded in 3.5wt% NaCl solution. Scan rate is 1.5 mV/s.

Table 4. Results of polarization curves of the AlCrN coatings corroded in 3.5 wt% NaCl solution.

Specimen	Corrosion current / $\mu\text{A cm}^{-2}$	Corrosion potential / mV	P (%)
Substrate	2.91	-346	—
120A	0.52	-288	82.23
150A	0.28	-229	90.52
180A	0.05	-165	98.25

Fig. 5 shows the potentiodynamic polarization curves of the substrate and AlCrN coatings deposited with different arc current in 3.5-wt% NaCl solution. Table 4 lists the electrochemical parameters measured by the curves. The corrosion potential (E_{corr}) of the substrate is about -346 mV. The AlCrN coatings revealed positive corrosion potential compared with the substrate. It means that deposited AlCrN coating has better corrosion resistance than the substrate. When the arc current of the deposited AlCrN coating is 120 A, 150A and 180A, the corrosion potential is -288 mV, -229mV and -165 mV respectively. This result shows that increasing the arc current obviously improves the corrosion resistance compared with the AlCrN coatings. The sample deposited at 180 A arc current has the highest corrosion resistance of all coating samples. Generally, the lower the corrosion current density (I_{corr}), the slower the corrosion rate. The corrosion current density is about $2.91 \mu\text{A cm}^{-2}$ for the substrate, and the corrosion current density decreases significantly for the deposited AlCrN coating, indicating that the corrosion rate of the AlCrN coating was lower than that of the substrate. It has been reported that transition metal nitride coatings have electrochemical inertness [31, 32]. In this study, the deposited AlCrN coating showed higher polarization resistance compared with 45 steel. In addition, the deposited AlCrN coating exhibited a nano-multilayer structure, which significantly inhibition of pitting corrosion expansion [33, 34]. For the samples deposited at 120 A, 150 A, and 180 A arc

currents, the corrosion current densities are $0.52 \mu\text{A cm}^{-2}$, $0.28 \mu\text{A cm}^{-2}$, and $0.05 \mu\text{A cm}^{-2}$ respectively. The decrease of corrosion current densities of deposited samples are mainly related to the formation of Al_2O_3 [9]. Compared the samples deposited at different arc currents, the sample with the current of 180A showed higher polarization resistance and lower corrosion rate which is due to the large arc current, and the increase of the Al content of the sample resulting in more Al_2O_3 . As shown in Table 4, the E_{corr} and I_{corr} values of the substrate were -346.7mV and $2.91 \mu\text{A cm}^{-2}$. The protection efficiency (P) was calculated as follows [35]:

$$P = (1 - I_{\text{corr}} / I_{\text{corr}}^0) \times 100\% \quad (1)$$

where I_{corr} and I_{corr}^0 are the corrosion current densities, present and absent of a coating, respectively. According to formula, the protective efficiency of the coating deposited on the substrate was more than 80%. Among them, the protective efficiency of as-deposited AlCrN coating with arc current of 180 A on the substrate reached 98.25%. These results indicated that the AlCrN coating deposited with 180A arc current has the best corrosion resistance to Cl ions, which is consistent with the Tafel curve shown in Fig. 5. Therefore, it can be concluded that the coating deposited at an arc current of 180 A was more suitable for industrial application.

4. CONCLUSION

The chemical compositions, surface morphologies, surface roughness, and corrosion resistance properties of AlCrN coatings at different arc currents were investigated. With the arc current increasing from 120 A to 180 A, the Al_8Cr_5 phase gradually changing the Cr (Al) N structure. The higher the arc currents, the thinner the coatings, so more substrate phases can be observed, and there are many metal droplets and particles on the coating surface. With the increase of arc current, the number and size of metal particles and droplets gradually decrease because of the melting of these solid metal droplets. Three-dimensional contour plots show that the surface roughness of the coating decreases with the increase of arc current. Among them, the roughness of the coating prepared with 180 A arc current is the lowest, which is $51.463 \text{ nm } R_a$. The result of potentiodynamic polarization curves shows that the AlCrN coating has better corrosion resistance than substrates. Then as the arc current increased, the corrosion resistance of the coating is also improved. When the arc current reached 180 A, the protection efficiency reached 98.25% in 3.5-wt% NaCl corrosion solution.

ACKNOWLEDGEMENTS

This research was financially supported by the Key R & D Projects of the Ministry of Science and Technology, China (No. 2016YFD0700903).

References

1. H. Cheng, X. Huang, H. Wang, *J. Mater. Process. Tech.*, 89 (1999) 339.
2. H. Liu, C. Wang, X. Zhang, *Surf. Coat. Tech.*, 228(S)(2013) s296.
3. G. Huang, L. Qu, Y. Lu, *Vacuum*, 153 (2018) 39.

4. J. Tuominen, J. Nakki, H. Pajukoski, *J. Laser. Appl.*, 27(2)(2015) 22009.
5. M. Van Stappen, L.M. Stals, M. Kerkhofs, *Surf. Coat. Tech.*, 629 (1995) 74.
6. C. S. Kumar, S. K. Patel, *Ceram. Int.*, 43 (2017) 13314.
7. M. Staszuk, L.A. Dobrzanski, T. Tanski, *Arch. Metall. Mater.*, 59 (1) (2014) 269.
8. M. Chen, D. Wu, W. Chen. *Thin Solid Films*, 612 (2016) 400.
9. K.C. Mutyala, H. Singh, R.D. Evans. *Surf. Coat. Tech.*, 305 (2016) 176.
10. S.H. Wan, J. B. Pu, D. S. Li, *J. Alloy. Comp.*, 695 (2017) 433.
11. Y. Chen, S. Wang, Y. Hao, *Tribol. Int.*, 143, (2020) 106079.
12. S. Wan, H. Wang, Y. Xia, *Wear*, 432 (2019) 202940.
13. W. Chen, J. Zheng, X. Meng, *Vacuum*, 121 (2015) 194.
14. J. Mo, M. Zhu, A. Leyland, *Surf. Coat. Tech.*, 215 (2013) 170.
15. J. Mo, M. Zhu, *Tribol. Int.*, 41 (2008) 1161.
16. M. Kawate, A.K. Hashimoto, T. Suzuki, *Surf. Coat. Tech.*, 165 (2003) 163.
17. J. Mo, M. Zhu, B. Lei, Y. Leng, N. Huang, *Wear*, 263 (2007) 1423.
18. A. Richter, *Cutting Tool Eng.*, 57 (2005) 10.
19. A.E. Reitera, V.H. Derflingera, B. Hanselmann, *Surf. Coat. Tech.*, 200 (2005) 2114.
20. K. M. Gupta, K. Ramdev, S. Dharmateja. *Proceedings*, 5 (2018) 11260.
21. J. Ramm, A. Neels, B. Widrig, *Surf. Coat. Tech.*, 205(5) (2010) 1356.
22. K. Mahdouk, J. C. Gachon, *J. Phase Equilib.*, 21 (2) (2000) 157.
23. M. Pohler, R. Franz, J. Ramm, P. Polcik, C. Mitterer, *Surf. Coat. Tech.*, 206 (6) (2011) 1454.
24. X. S. Wan, S. S. Zhao, Y. Yang, J. Gong, C. Sun, *Surf. Coat. Tech.*, 204 (2010) 1800.
25. V. K. W. Grips, H. C. Barshilia, V. E. Selvi, *Thin Solid Films.*, 514 (2006) 204.
26. R. Ananthakumar, B. Subramanian, A. Kobayashi, *Ceram. Int.*, 38 (2012) 477.
27. F. Cai, S. Zhang, J. Li, *Appl. Surf. Sci.*, 258 (2011) 1819.
28. Y. Feng, L. Zhang, R. Ke, *Int. J. Refract. Met. Hard. Mater.*, 43 (2014) 241.
29. T. Mashiki, H. Hikosaka, H. Tanoue, *Thin Solid Films*, 516 (2008) 6650.
30. P. Cisquini, S. V. Ramos, P. R. P. Viana, *jmr&t*, 8(2) (2019) 1897.
31. L. Cunha, M. Andritschky, *Surf. Coat. Tech.*, 111 (1999) 158.
32. S. B. Abusuilik, K. Inoue, *Surf. Coat. Tech.*, 237 (2013) 421.
33. V. K. W. Grips, H. C. Barshilia, V. E. Selvi, K.S.R. Kalavati, *Thin Solid Films*, 514 (2006) 204.
34. N. E. Beliardouh, K. Bouzid, C. Nouveau, *Tribol. Int.*, 82 (2015) 443.
35. N. D. Nam, M. Vaka, N. T. Hung, *J. Power Sources*, 268 (2014) 240.